Competition between Triborane as a Ligand and a Hydride Donor at Platinum Centres containing Chelating Phosphines: Molecular Structures of $[\{Ph_2P(CH_2)_2PPh_2\}PtB_3H_7]$, $[\{Ph_2P(CH_2)_4PPh_2\}PtB_3H_7]$ and $[Pt_2H_3\{(Ph_2PC_5H_4)_2Fe\}_2]Cl$†

Brian S. Haggerty,[a] Catherine E. Housecroft,*[,b] Arnold L. Rheingold*[,a] and Bilal A. M. Shaykh[b]

[a] *Department of Chemistry, University of Delaware, Newark, DE 19716, USA*

[b] *University Chemical Laboratory, Lensfield Road, Cambridge CB2 1EW, UK*

The reaction of $[PtCl_2(L\text{–}L)]$ [L–L = $Ph_2P(CH_2)_nPPh_2$, n = 2, 3 or 4; or $Fe(\eta^5\text{-}C_5H_4PPh_2)_2$] with the octahydrotriborate(1−) anion, $[B_3H_8]^-$, leads to both $[(L\text{–}L)PtB_3H_7]$ in which the borane unit acts as a pseudo-bidentate ligand and $[Pt_2H_3(L\text{–}L)_2]Cl$ which results from the borane anion functioning as a hydride donor. For each of the complexes containing a bis(diphenylphosphino)alkane ligand the major product is $[\{Ph_2P(CH_2)_nPPh_2\}PtB_3H_7]$, whereas for the reaction of $[B_3H_8]^-$ with $[Fe(\eta^5\text{-}C_5H_4PPh_2)_2]$, $[Pt_2H_3\{(Ph_2PC_5H_4)_2Fe\}_2]Cl$ is the predominant species formed. Three products have been structurally characterised: $[\{Ph_2P(CH_2)_2PPh_2\}PtB_3H_7]$ **1**, space group $P2_1/c$, a = 16.049(4), b = 15.395(4), c = 21.075(5) Å, β = 90.53(2)°, Z = 8, R = 0.039; $[\{Ph_2P(CH_2)_4PPh_2\}PtB_3H_7]$ **3**, space group $P2_1$, a = 8.8826(18), b = 17.7329(32), c = 9.5520(17) Å, β = 114.115(15)°, Z = 2, R = 0.032; $[Pt_2H_3\{(Ph_2PC_5H_4)_2Fe\}_2]Cl\cdot 3CH_2Cl_2$ **6**, space group $P2_1/c$, a = 12.862(2), b = 38.732(6), c = 14.271(2) Å, β = 99.027(15)°, Z = 4, R = 0.067. The structure of the cation of **6** resembles that of $[Pt_2(\mu\text{-}H)_2H\{Ph_2P(CH_2)_2PPh_2\}_2]^+$ rather than that of $[Pt_2(\mu\text{-}H)H_2\{Bu^t_2P(CH_2)_3PBu^t_2\}_2]^+$ thereby indicating that it is the steric bulk of the phosphorus substituents rather than the P–Pt–P bite angle that controls the geometry of the $\{Pt_2P_4\}$ framework and thus the hydride locations. Fenske–Hall molecular orbital calculations have been used to probe the mode of bonding of the hydride ligands to the diplatinum centre.

As part of a series of studies relating to the reactivity of the octahydrotriborate(1−) anion with complexes of the type $[MCl_2(L\text{–}L)]$ [L–L = chelating bis(phosphine); M = Group 10 transition metal] we recently reported the synthesis and characterisation of the palladatetraboranes $[\{Ph_2P(CH_2)_n\text{-}PPh_2\}PdB_3H_7]$ (n = 1–4)[1] and $[\{(Ph_2PC_5H_4)_2Fe\}PdB_3H_7]$.[2] In each case the metallaborane represented the only isolated palladium-containing species. By-products were the adducts $H_3B(L\text{–}L)BH_3$, Et_3NBH_3 and $Et_3NB_3H_7$, the amine arising from the solvent mixture.[1–3] We now report the reactivity of the octahydrotriborate(1−) anion towards platinum(II) dichloride complexes that contain chelating bis(phosphine) ligands. In addition to observing the expected platinatetraborane complexes, $[(L\text{–}L)PtB_3H_7]$,[3,4] we have found that a competitive pathway (Scheme 1) is the formation of both mononuclear and dinuclear platinum(II) hydride complexes with those of general formula $[Pt_2H_3(L\text{–}L)_2]^+$ being preferred. Diplatinum hydrides of this family have previously been prepared from mononuclear platinum hydride complexes,[5–9] by oxidative addition of methanol to dimeric platinum(0) complexes,[6] or by treatment of $[Pt(Hdmpz)_2(L\text{–}L)]^{2+}$ (Hdmpz = 3,5-dimethylpyrazole) or $[Pt_2(OH)_2(L\text{–}L)_2]^{2+}$ with $[BH_4]^-$,[10,11] the latter being a more potent hydride donor than $[B_3H_8]^-$. In general, the reaction of the $[B_3H_8]^-$ ion with a transition-metal halide leads to a metalloborane containing a bi- or tri-dentate $\{B_3H_8\}$ ligand or a 'π-allyl' $\{B_3H_7\}$ ligand.[12] Examples in which a metal–hydride bond is also formed are $[(OC)_3HFeB_3H_8]$,[13] $[(Ph_3P)_2(OC)\text{-}HIrB_3H_7]$,[14,15] and $[(Ph_3P)_2H_2IrB_3H_8]$,[16] while in the reaction of $[Ir(dppe)_2]^+$ (dppe = $Ph_2PCH_2CH_2PPh_2$) with $[B_3H_8]^-$ the only product is the hydride species $[IrH_2\text{-}(dppe)_2]^+$.[14] It has been suggested that the hydride ligand required for the formation of $[(OC)_3HFeB_3H_8]$ may arise from the decomposition of a bis(octahydrotriborato)iron complex.[13] Although the synthesis of some platinatetraboranes from $[PtCl_2L_2]$ and $[B_3H_8]^-$ [L = PPh_3, PEt_3, $PPhMe_2$, or $P(C_6H_4Me\text{-}p)_3$] has previously been reported,[3,4] the competitive formation of platinum hydride complexes during such reactions has not, to our knowledge, been observed until now.

Experimental

Manipulations were carried out under an inert atmosphere using standard Schlenk techniques.[17] Solvents were dried over suitable reagents, degassed and distilled before use. The compound $PtCl_2$ (Johnson Matthey), dppe, dppp $[Ph_2P\text{-}(CH_2)_3PPh_2]$, dppb $[Ph_2P(CH_2)_4PPh_2]$ and $[Fe(\eta^5\text{-}C_5H_4PPh_2)_2]$ (Aldrich), and $[NMe_4][B_3H_8]$ (Alfa-Ventron) were used as received. Column chromatography used Kieselgel (70–230 mesh) (Merck). The complexes $[PtCl_2(L\text{–}L)]$ were prepared following the literature method reported for the synthesis of $[PtCl_2\{Ph_2P(CH_2)_nPPh_2\}]$ (n = 1–3).[18] FT-NMR spectra were recorded on a Brüker AM 400 spectrometer. Proton NMR chemical shifts are with respect to δ = 0 for $SiMe_4$, ^{11}B NMR with respect to δ = 0 for $F_3B\cdot OEt_2$, and ^{31}P NMR with respect to δ = 0 for 85% H_3PO_4(aq). All downfield chemical shifts are positive. Infrared spectra were

† 1-[1,2-Bis(diphenylphosphino-κ*P*)ethane]-1-platina- and 1-[1,4-bis-(diphenylphosphino-κ*P*)butane]-1-platina-*arachno*-tetraborane(7), and tetrakis(μ-diphenylphosphinocyclopentadienyl)-1(η^5):2κ*P*; 1(η^5):2κ*P*; 3κ*P*:4(η^5); 3κ*P*:4(η^5)-di-μ-hydrido-2:3κ²*H*-hydrido-2κ*H*-diiron-diplatinum chloride.

Supplementary data available: see Instructions for Authors, *J. Chem. Soc., Dalton Trans.*, 1991, Issue 1, pp. xviii–xxii.

Non-S.I. unit employed: eV ≈ 1.60 × 10^{-19} J.

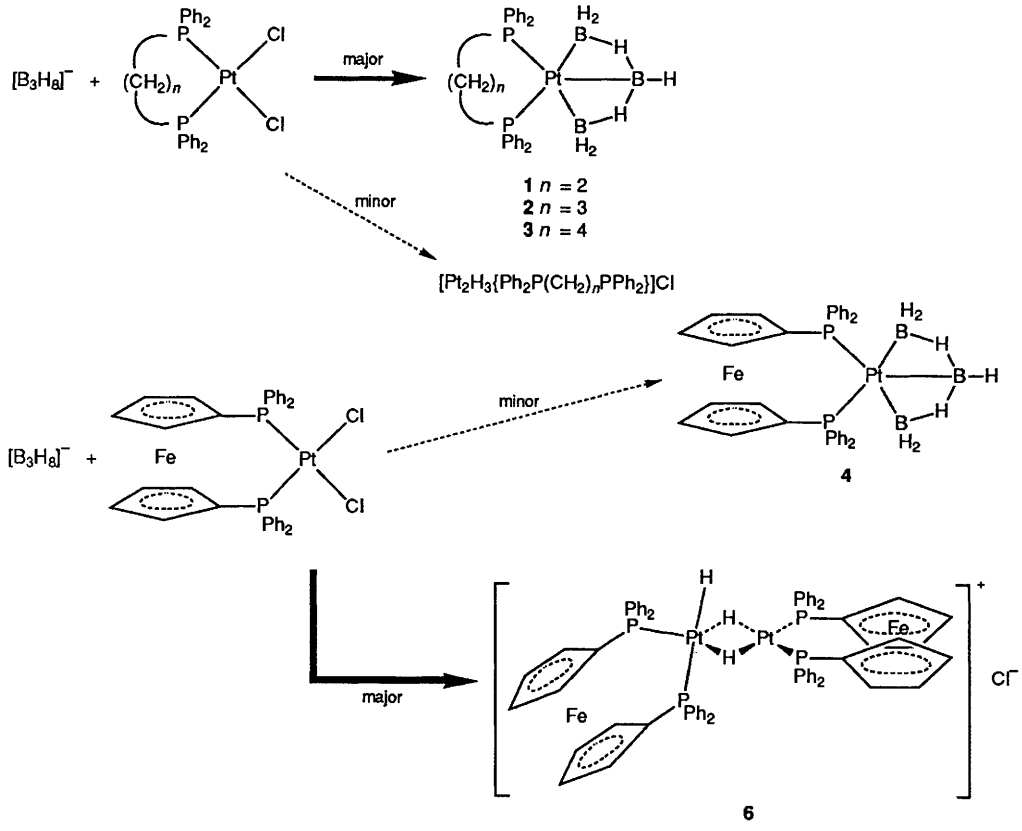

Scheme 1

recorded on a Perkin-Elmer FT 1710 spectrophotometer, fast atom bombardment (FAB) mass spectra (*p*-nitrobenzyl alcohol matrix) on a Kratos MS 890 instrument.

Preparations.—[(dppe)PtB_3H_7] **1**. The method of synthesis was adapted from that reported by Muetterties and co-workers[3] for [$(Ph_3P)_2PtB_3H_7$]. In a typical reaction, [NMe_4][B_3H_8] (0.12 g, 1.0 mmol) was added to a solution of [$PtCl_2$(dppe)] (0.66 g, 1.0 mmol) in MeCN (100 cm^3) and NEt_3 (25 cm^3). The mixture was stirred for 5 h. The salt [NMe_4]Cl was precipitated and the supernatant was removed by cannula; solvent was removed *in vacuo* to give a grey crude residue. Column chromatography eluting with hexanes separated Et_3NBH_3 and $Et_3NB_3H_7$ which were identified by ^{11}B and ^1H NMR and mass spectroscopy. Further elution using toluene gave compound **1** as the first band (yield ≈25%). FAB mass spectrum: *m/z* 634 (P^+) and 620 ($P^+ - BH_3$). NMR spectroscopic data are listed in Table 1.

[(dppp)PtB_3H_7] **2**. Crude compound **2** was prepared on a 1.0 mmol scale by the method described for **1**. Column chromatography eluting with hexanes separated Et_3NBH_3 and $Et_3NB_3H_7$. Following this, elution with toluene separated **2** in 20% yield. Further elution using methanol separated [Pt_2H_3(dppp)$_2$]Cl **5** (≈2% yield) as the first band, and a mixture of [PtH(Cl)(dppp)] and [$PtH(dppp)_2$]Cl (< 1% yield) as the second fraction. [(dppp)PtB_3H_7]: FAB mass spectrum *m/z* 648 (P^+), 634 ($P^+ - BH_3$) and 607 ($P^+ - B_3H_7$); NMR spectroscopic data in Table 1. [$Pt_2H_3(dppp)_2]^+$: ^{31}P and ^1H NMR data agreed with those previously published;[10] FAB mass spectrum *m/z* 1217 (P^+). The compound [PtH(Cl)(dppp)] and the [$PtH(dppp)_2]^+$ cation were characterised on the basis of their high-field hydride resonances. 400 MHz ^1H NMR (CD_2Cl_2, 298 K): [PtH(Cl)(dppp)], δ −3.67 (qnt, J_{PH} = 39) with ^{195}Pt satellites (J_{PtH} = 456); [$PtH(dppp)_2]^+$, δ −4.38 (dd, $J_{PH_{trans}}$ = 157, $J_{PH_{cis}}$ = 17) with ^{195}Pt satellites (J_{PtH} = 875 Hz).

[(dppb)PtB_3H_7] **3**. Crude compound **3** was prepared on a 1.0 mmol scale by the method described for **1**. Column chromatographic separation used first hexanes to remove Et_3NBH_3 and $Et_3NB_3H_7$, and secondly toluene to give **3** (≈20% yield). [(dppb)PtB_3H_7]: FAB mass spectrum *m/z* 661 (P^+), 647 ($P^+ - BH_3$) and 621 ($P^+ - B_3H_7$); NMR spectroscopic data in Table 1.

[Pt_2H_3{$(Ph_2PC_5H_4)_2Fe$}$_2$]Cl **6**. An attempt was made to prepare [{$(Ph_2PC_5H_4)_2Fe$}PtB_3H_7] **4**, by the method described for compound **1**. Spectroscopic characterisation of the crude mixture showed the presence of **6** as the primary product and minor (≈2% by ^{31}P NMR data) amounts of **4**. The platinaborane proved to be elusive on separation of the crude mixture by column chromatography; isolation of **6** was achieved by washing the crude product with methanol and recrystallising the residue from a CH_2Cl_2–hexanes–Et_2O mixture (yield ≈10%). The ^{31}P and ^1H NMR data for the chloride agreed with those already published for the tetrafluoroborate salt;[11] FAB mass spectrum *m/z* 1501 (P^+) and 749 [$P^+ - PtH_3${$(Ph_2PC_5H_4)_2Fe$}].

Crystal Structure Determination of [(dppe)PtB_3H_7] **1**, [(dppb)PtB_3H_7] **3** *and* [Pt_2H_3{$(Ph_2PC_5H_4)_2Fe$}$_2$]Cl **6**.—Crystallographic data for compounds **1**, **3** and **6** are collected in Table 2. All specimens were mounted on glass fibres. Photographic evidence and systematic absences in the diffraction data determined 2/*m* Laue symmetry for all crystals. For **1** and **6** the space group was uniquely determined; for **3** either $P2_1$ or $P2_1/m$ was possible. While mirror-plane symmetry is potentially possible for **3**, the location of the molecule in the lattice, the asymmetry of the alkyl chain connecting the phosphorus atoms and the computational stability of the model during refinement all indicated that the non-centrosymmetric choice, $P2_1$, was correct. Empirical absorption corrections were applied to all data sets. A correction for a small (3%) linear decay in the intensities of the check reflections for **6** was applied.

The structures were all solved by direct methods. During refinement all phenyl rings were constrained to rigid, planar hexagons. Hydrogen atoms were placed in idealised locations,

Table 1 128 MHz ^{11}B, 162 MHz ^{31}P and 400 MHz ^{1}H spectroscopic data for complexes **1–3**

Compound	$\delta(^{11}B)$ (J_{PtB}/Hz) (at 298 K in CD_2Cl_2)	$\delta(^{31}P)$ (J_{PtP}/Hz) (at 298 K in CD_2Cl_2)	$\delta(^{1}H)$ (at 203 K in CD_2Cl_2)
1 [(dppe)PtB_3H_7]	+19.4 (1B, 500 ± 25) +3.7 (2B)	+55.0 (2537)	−2.74 (2 H, br, BHB), +2.75 (2 H, br, BH), +3.10 (1 H, br, BH), +4.15 (2 H, br, BH)
2 [(dppp)PtB_3H_7]	+19.4 (1B, 525 ± 25) +3.5 (2B)	+7.0 (2573)	−2.85 (2 H, br, BHB), +2.38 (2 H, br, BH), +3.14 (1 H, br, BH), +3.35 (2 H, br, BH)
3 [(dppb)PtB_3H_7]	+19.5 (1B, 525 ± 25) +3.5 (2B)	+23.0 (2693)	−2.87 (2 H, br, BHB), +1.92 (2 H, br, BH), +3.00 (1 H, br, BH), +3.20 (3 H, br, BH)
[{$(Ph_2PC_5H_4)_2Fe$}PtB_3H_7]	*a*	+28.0 (2790)	−2.88 (2 H, br, BHB)[b]

[a] Quantity too small for resolved ^{11}B NMR spectrum. [b] Resonances for terminal H atoms were not assigned due to inability to separate this compound.

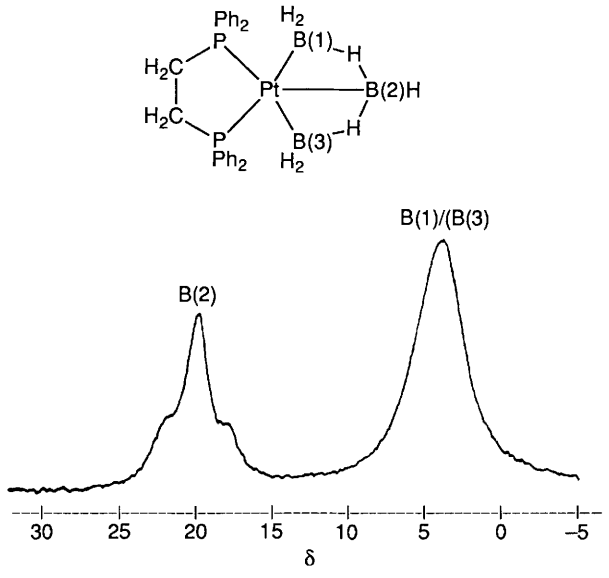

Fig. 1 The ^{11}B-{^{1}H} NMR spectrum for complex **1** showing the ^{11}B–^{195}Pt coupling for atom B(2); the inset diagram carries the same numbering scheme as that in Fig. 2

except for those bound to either metal or boron atoms, in which case they were ignored due to positional uncertainty. All non-hydrogen atoms were refined with anisotropic thermal parameters. For **3**, a multiplicative term, η, for $\Delta f''$ was refined to determine the correct hand; for the one reported, $\eta = 0.96(3)$ indicating that it is correct.

The software used for all calculations was SHELXTL 5.1.[19]

Additional material available from the Cambridge Crystallographic Data Centre comprises H-atom coordinates, thermal parameters, and remaining bond lengths and angles.

Molecular-orbital Calculations.—Fenske–Hall[20] calculations used the crystallographically determined coordinates of the {Pt_2P_4} core of cation **6** with Pd replacing Pt atoms to reduce the atomic orbital basis set. Each $(Ph_2PC_5H_4)_2Fe$ ligand was replaced by two PH_3 groups with the P–H bonds (1.41 Å) directed along the P–C vectors; Pd–H distances of 1.60 Å for a terminal bond and 1.92 Å for a fully bridging interaction were chosen. Single-ζ Slater functions were employed for the 1s and 2s functions of B, C and P. The exponents were obtained by curve fitting the double-ζ functions of Clementi[21] while maintaining orthogonal functions. The double-ζ functions were used directly for the 2p orbitals. For P an expanded atomic basis set used an exponent for the 3d functions of 1.8. An exponent of 1.16 was used for hydrogen. The palladium functions were augmented by 5s and 5p functions with exponents of 2.20.[22] Fragment orbital energies (see Fig. 8) are taken from the self-consistent field matrix of the final complex.[23]

Results and Discussion

The reaction of a bis(diphenylphosphino)alkane-palladium(II) or -platinum(II) dichloride with the octahydrotriborate(1−) anion is a convenient method of introducing a triborane ligand, {B_3H_7}, on to the palladium or platinum centre. The presence of a *short* alkane chain ($n \leqslant 4$ for Pd[1] and $n \leqslant 5$ for Pt) allows the bis(phosphine) ligand to participate in a chelate ring, thus rendering the chloride ligands mutually *cis*. Longer alkane backbones in the $Ph_2P(CH_2)_nPPh_2$ ligand favour dimerisation of the starting dichloride with the formation of *trans*-[{MCl_2(L–L)}$_2$] (M = Pd or Pt).[1,24] A *cis* arrangement of the two chlorine atoms appears to be a prerequisite for reaction with the octahydrotriborate(1−) anion,[1] although it has been shown that *trans*-[PtH(Cl)$(PEtPh_2)_2$] and *trans*-[IrH(CO)$(PPh_3)_2$] react with $[B_3H_8]^-$ to give $[(Ph_2EtP)_2PtB_3H_7]$[3] and $[(Ph_3P)_2(OC)HIrB_3H_7]$[14] respectively. We have also found that the use of one bidentate rather than two monodentate phosphine ligands is advantageous since it reduces complex fragmentation and the formation of phosphine boranes during reaction.

For each of the phosphine ligands, dppe, dppp and dppb, ^{11}B, ^{31}P and ^{1}H NMR spectroscopic data (see Table 1) for the crude reaction mixture of [$PtCl_2$(L–L)] with $[B_3H_8]^-$ indicate that a platinaborane complex, **1–3** respectively (Scheme 1), is the primary product. For the $Fe(\eta^5\text{-}C_5H_4PPh_2)_2$ ligand, ^{31}P and ^{1}H NMR spectroscopic data indicate that compound **4** is only generated in *ca.* 2% yield. This low yield and our inability to purify **4** precluded any further investigation of this compound. The solution NMR spectroscopic characteristics of each of complexes **1–3** are similar to those of their palladium analogues.[1] Each platinatetraborane exhibits signals in the ^{11}B NMR spectrum at *ca.* δ +19.4 (1 B) and 3.6 (2 B). Satellites due to ^{11}B–^{195}Pt spin coupling are clearly observed for the central boron atom, B(2) (Table 1), but the inherent linewidth of the higher-field resonance masks any such coupling pattern for atoms B(1) and B(3) (Fig. 1). The ^{1}H NMR spectral signatures of compounds **1–3** at room temperature show that in each case the borane has a static structure in solution on the 400 MHz time-scale. This is consistent with the solution properties of [(L–L)PdB_3H_7] [L–L = dppm $(Ph_2PCH_2PPh_2)$,[1] dppe,[1,3] dppp,[1] dppb,[1] or $Fe(\eta^5\text{-}C_5H_4PPh_2)_2$[1,2]] [$L_2PtB_3H_7$] [L = PPh_3, PEt_3, $PPhMe_2$ or $P(C_6H_4Me\text{-}p)_3$][3,4] and $[(Ph_3P)_2(OC)HIrB_3H_7]$.[14] The region of the spectrum attributable to the bridging hydrogen atoms is almost unchanged across this series of compounds. At room temperature, resolution of the three types of $BH_{terminal}$ protons (ratio 2:2:1) is not apparent; in the case of **2** this is due to an overlap of resonances for $BH_{terminal}$ and methylene protons. Thermal decoupling of the ^{11}B–^{1}H spins[25] at 203 K allows resolution of the resonances in the cases of compounds **1** and **3**, but the signals remain unresolved for **2**. By using ^{11}B–^{1}H NMR chemical shift correlation experiments the presence of the three types of $BH_{terminal}$ protons can be confirmed for each of **1–3** as shown in Table 1. Note that the spectroscopic data imply that, in solution, the {B_3H_7} moiety is

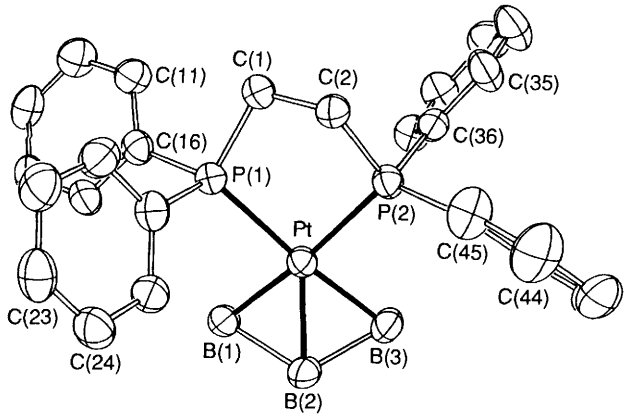

Fig. 2 Molecular structure and atom labelling for complex **1**. Hydrogen atoms were not located

Table 2 Crystal data for compounds **1**, **3** and **6***

(*a*) Crystal parameters			
Formula	$C_{26}H_{31}B_3P_2Pt$	$C_{28}H_{35}B_3P_2Pt$	$C_{68}H_{59}ClFe_2P_4Pt_2{\cdot}3CH_2Cl_2$
M	632.96	660.97	1792.12
Space group	$P2_1/c$	$P2_1$	$P2_1/c$
a/Å	16.049(4)	8.8826(18)	12.862(2)
b/Å	15.395(4)	17.7329(32)	38.732(6)
c/Å	21.075(5)	9.5520(17)	14.271(2)
β/°	90.53(2)	114.115(15)	99.027(15)
U/Å^3	5206.9(23)	1372.2(4)	7021.1(2)
Z	8	2	4
Crystal dimensions/mm	0.31 × 0.32 × 0.34	0.29 × 0.30 × 0.36	0.26 × 0.31 × 0.36
Crystal colour	Colourless	Colourless	Gold-yellow
D_c/g cm^{-3}	1.615	1.600	1.695
μ(Mo-Kα)/cm^{-1}	58.0	55.0	47.8
F(000)	2480	652	3408
T/K	297	296	295
T(max.)/T(min.)	3.2	1.38	1.84
(*b*) Data collection			
2θ Scan range/°	4–48	4–60	4–48
Data collected, (h, k, l)	±19, +18, +25	±13, +25, +14	±16, +47, +17
Reflections collected	8784	4348	11 868
Independent reflections	8176	4119	11 130
R(merg)	0.023	0.018	0.058
Independent observed reflections	5871	3553	5210
[$F_o \geqslant n\sigma(F_o)$]	(n = 4)	(n = 4)	(n = 3)
Variation in standards (%)	<1	<1	3
(*c*) Refinement			
R	0.039	0.032	0.067
R'	0.041	0.033	0.065
Δ/σ(max.)	0.05	0.07	0.13
Δ(ρ)/e Å^{-3}	1.24	1.26	1.26
N_o/N_v	10.9	13.5	8.0
Goodness of fit	1.062	1.000	1.416

* Details in common: monoclinic; Nicolet R3m/μ diffractometer with graphite monochromator; Mo-Kα radiation (λ = 710 73 Å); three standards per 197 reflections. Weighting scheme $w^{-1} = [\sigma^2(F_o) + 0.001(F_o)^2]$

bound in a symmetrical environment in each platinatetraborane.

The molecular structures of compounds **1** and **3** have been determined and, together with that of [{$(Ph_2PC_5H_4)_2Fe$}-PdB_3H_7],[2] illustrate the ability of the co-ordinated triborane ligand to tolerate changes in the steric requirements of the chelating bis(diphenylphosphino) ligand. Each of **1** and **3** may be described either in terms of a pseudo-square-planar co-ordination complex or an *arachno*-metallaborane cluster. In the former description the two phosphorus donor atoms occupy two co-ordination sites which are mutually *cis* and the 'π-allyl' B_3H_7 ligand spans the remaining two sites.[3,4,26] In the latter description the [$Ph_2P(CH_2)_nPPh_2$]Pt unit acts as a three-electron fragment occupying one 'hinge' site of an *arachno*-PtB_3 butterfly cluster.[1,15]

The molecular structure of compound **1** is shown in Fig. 2 and selected bond lengths and angles are listed in Table 4. The triborane(7) unit resides symmetrically with respect to the [bis(diphenylphosphino)ethane] platinum(II) fragment and this is seen clearly in the schematic structure in Fig. 3(*a*). The internal dihedral angle of the PtB_3 butterfly is 133.4° and this is larger than the value of 127.3° in [$(Me_2PhP)_2PtB_3H_7$],[3] 129.4° in [{$(Ph_2PC_5H_4)_2Fe$}PdB_3H_7],[2] 126.5° in [$(Ph_3P)_2$(OC)-$HIrB_3H_7$],[15] or 124.5 (by electron diffraction)[27] or 117.4° (by microwave spectroscopy)[28] in B_4H_{10}. The three boron atoms are all within bonding distance of the platinum atom with the central boron atom being closer [2.119(12) Å] than the other two [2.173(12) and 2.160(13) Å]. The direct interaction implied by the distance Pt–B(2) in particular is consistent with the value of the ^{11}B–^{195}Pt coupling constant observed in the ^{11}B NMR spectrum (Fig. 1). The {(dppe)Pt} fragment of the molecule is unexceptional; the methylene groups of the dppe chain are disposed symmetrically, one above and one below, the PtP_2 plane. The bite angle, P(1)–Pt–P(2), of 85.3(1)° is close to that observed in the starting complex [$PtCl_2$(dppe)] [86.3(2)[29] and 86.72(6)°[30]] and is also consistent with a value of 85.82(7)° in the analogous [$PdCl_2$(dppe)].[31] In a comparative study of the structures of [$PdCl_2$(dppm)], [$PdCl_2$(dppe)] and [$PdCl_2$-(dppp)], Steffen and Palenik[31] have illustrated that it is the dppe ligand that forms the least-strained complex. Using the PMP angle as a means of testing the degree of strain in compound **1**, we suggest that the symmetrical siting of the B_3H_7 fragment with respect to the P_2Pt unit follows from the fact that the molecule experiences little or no strain.

Fig. 4 illustrates the molecular structure of compound **3**; selected bond lengths and angles are listed in Table 6. In this structure atom B(2) is disordered, with a 71% occupancy in the site shown in Fig. 4 [namely, B(2) lies on the same side of the P_2Pt plane as does the carbon chain of the dppb ligand] and a 29% occupancy with B(2) lying on the opposite side of the P_2Pt plane. Schematic representations of the structure which highlight the orientations of both the borane unit and the alkane backbone of dppb are shown in Figs. 3(*b*) (71% occupancy) and 3(*c*) (29% occupancy). Two structural features are worth comment. First, the alkane chain of the dppb ligand is folded towards one side of the pseudo-square-planar co-ordination sphere of the platinum atom. Secondly, the triborane(7) unit is skewed with respect to the PtP_2 plane in contrast to the symmetrical environment noted in **1**. The B_3H_7 moiety may respond to an increase in the bite angle of the bis(diphenylphosphine) ligand by either twisting out of plane or by decreasing the internal dihedral angle of the B_3 butterfly. However, a comparison of the geometrical parameters of compounds **1** and **3** with those of [{$(Ph_2PC_5H_4)_2Fe$}PdB_3H_7][2] shows *no* trend between the steric requirements of the bis(phosphine) ligand and changes in the two aforementioned geometrical parameters of the B_3 butterfly. Hence, we conclude that the asymmetric placement of the B_3H_7 unit in **3** is due simply to packing forces. This result supports one made earlier for [{$(Ph_2PC_5H_4)_2Fe$}PdB_3H_7].[2]

Preliminary ^1H NMR spectroscopic data for the crude product mixture from the reaction of [$PtCl_2$(dppp)] with the octahydrotriborate(1−) anion suggested that, in addition to the formation of a metallaborane complex, there is a competitive route in which the borane anion acts as a hydride donor rather than as a potential ligand. For the dppp complex minor

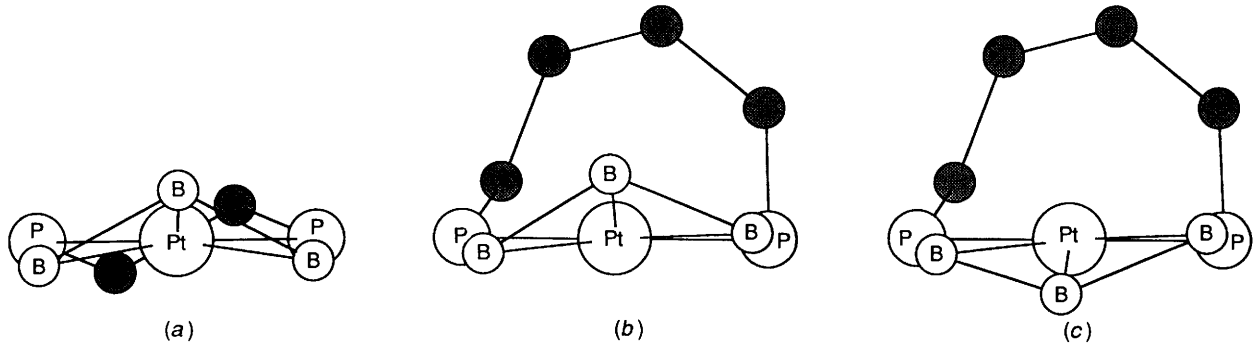

Fig. 3 Schematic representations of complexes **1** and **3** viewed through the PtP_2 plane: (*a*) **1**, (*b*) **3** for B(2) in the site with 71% occupancy, and (*c*) **3** for B(2) in the site with 29% occupancy

Table 3 Atomic coordinates ($\times 10^4$) for complex **1**

Atom	*x*	*y*	*z*	Atom	*x*	*y*	*z*
Pt	1677.7(2)	6645.9(2)	6292.6(2)	C(26)	3018	7074	7541
Pt′	3384.4(2)	1917.6(2)	4718.1(2)	C(31)	1116(4)	8266(4)	5169(3)
P(1)	2227(2)	7581(2)	7040(1)	C(32)	695	8898	4817
P(2)	2516(2)	7365(2)	5588(1)	C(33)	1127	9408	4383
P(1′)	2679(2)	2767(2)	4005(1)	C(34)	1981	9285	4300
P(2′)	2554(2)	2548(2)	5466(1)	C(35)	2402	8652	4653
B(1)	787(7)	6125(8)	6963(5)	C(36)	1969	8143	5087
H(a)	933(43)	5874(46)	7438(33)	C(41)	2799(3)	6332(4)	4533(3)
H(c)	492(74)	5514(76)	6685(52)	C(42)	3270	5800	4138
B(2)	1109(8)	5404(8)	6310(5)	C(43)	4121	5694	4254
H(d)	1542(60)	4744(69)	6443(45)	C(44)	4501	6121	4764
H(e)	648(46)	5328(49)	5745(34)	C(45)	4030	6653	5158
B(3)	1088(9)	5905(8)	5543(6)	C(46)	3178	6758	5042
H(f)	1255(43)	5548(46)	5228(32)	C(11′)	4063(4)	3480(4)	3411(3)
H(g)	348(63)	6361(67)	5404(47)	C(12′)	4467	3944	2936
B(1′)	4264(8)	1392(9)	4027(6)	C(13′)	4010	4296	2432
H(a′)	4668(115)	1796(112)	3848(84)	C(14′)	3148	4184	2403
H(c′)	3996(69)	880(75)	3651(52)	C(15′)	2743	3719	2877
H(d′)	5059(122)	1701(117)	4970(89)	C(16′)	3201	3367	3382
B(2′A)	4045(16)	699(17)	4628(12)	C(21′)	2176(3)	1527(4)	3150(3)
B(2′B)	4572(15)	1216(17)	4869(12)	C(22′)	1613	1012	2810
B(3′)	3939(12)	1080(15)	5431(6)	C(23′)	758	1120	2894
H(f′)	3915(45)	1024(48)	5807(33)	C(24′)	467	1743	3319
C(1)	2766(6)	8434(6)	6615(4)	C(25′)	1030	2257	3659
C(2)	3246(6)	8036(6)	6060(4)	C(26′)	1885	2149	3575
C(1′)	2113(6)	3622(6)	4439(4)	C(31′)	3524(4)	2832(3)	6530(3)
C(2′)	1781(6)	3268(6)	5071(4)	C(32′)	4001	3321	6956
C(11)	1553(4)	9052(4)	7651(3)	C(33′)	4067	4218	6878
C(12)	1132	9457	8146	C(34′)	3656	4626	6373
C(13)	779	8959	8627	C(35′)	3179	4137	5947
C(14)	847	8056	8612	C(36′)	3113	3240	6026
C(15)	1269	7651	8118	C(41′)	1745(4)	1025(4)	5796(3)
C(16)	1622	8149	7637	C(42′)	1192	525	6149
C(21)	3545(4)	7576(3)	7924(3)	C(43′)	783	891	6665
C(22)	4077	7174	8361	C(44′)	927	1757	6828
C(23)	4083	6271	8415	C(45′)	1480	2257	6475
C(24)	3556	5769	8033	C(46′)	1889	1890	5959
C(25)	3024	6171	7596				

Table 4 Selected bond lengths (Å) and angles (°) for complex **1**

Pt–P(1)	2.304(2)	Pt–P(2)	2.297(2)
Pt–B(1)	2.173(12)	Pt–B(2)	2.119(12)
Pt–B(3)	2.160(13)	B(1)–B(2)	1.846(16)
B(2)–B(3)	1.791(17)	P(1)–C(16)	1.821(6)
P(1)–C(26)	1.819(7)	P(2)–C(36)	1.818(7)
P(2)–C(46)	1.829(7)	P(2)–C(2)	1.845(9)
C(1)–C(2)	1.535(13)	P(2)–C(1)	1.813(10)
P(1)–Pt–P(2)	85.3(1)	B(1)–Pt–B(3)	89.7(5)
B(1)–Pt–B(2)	50.9(4)	B(2)–Pt–B(3)	49.5(5)
B(1)–B(2)–B(3)	114.3(8)	Pt–P(1)–C(1)	107.2(3)
P(1)–C(1)–C(2)	109.4(3)	Pt–P(2)–C(2)	107.1(3)
P(2)–C(2)–C(1)	108.3(3)		

amounts of $[Pt_2H_3(dppp)_2]Cl$ **5** (≈2% yield), [PtH(Cl)-(dppp)] and $[PtH(dppp)_2]Cl$ (<1% yield) are formed. The last two hydride complexes were not isolated but were identified by their diagnostic signatures in the ^1H NMR spectrum. Related species are $[NiH(dppe)_2]^+$ [32] and [PtH(Cl)-{$C_6H_4(CH_2PPh_2)$-1,2}] [33] Compound **5** was separated and its identity confirmed from its mass spectrum and by comparison of ^1H and ^{31}P NMR spectral properties with those of $[Pt_2H_3(dppp)_2][BF_4]$.[10]

In contrast to any of the other bis(phosphine)-platinum(II) or palladium(II) dichlorides that we have investigated here or previously,[1,2] and significantly this includes $[PdCl_2\{(Ph_2PC_5H_4)_2Fe\}]$ [2], $[PtCl_2\{(Ph_2PC_5H_4)_2Fe\}]$ predominantly sees the octahydrotriborate(1−) anion as a source of H^- rather than as

Table 5 Atomic coordinates ($\times 10^4$) for complex **3**

Atom	*x*	*y*	*z*	Atom	*x*	*y*	*z*
Pt	9 621.6(3)	2 500	1 338.1(2)	C(22)	6 641	4 161	−3 396
P(1)	9 939(2)	2 546(3)	−947(2)	C(23)	5 665	3 797	−4 761
P(2)	8 547(3)	1 284(1)	954(2)	C(24)	5 992	3 050	−4 999
B(1)	9 464(13)	2 499(13)	3 570(9)	C(25)	7 296	2 666	−3 870
B(2)	10 957(20)	3 112(10)	3 401(18)	C(26)	8 273	3 030	−2 504
B(2′)	9 463(23)	3 418(15)	2 705(23)	C(31)	6 489(6)	1 084(3)	2 479(5)
B(3)	10 414(21)	3 679(8)	1 797(13)	C(32)	6 131	871	3 716
C(1)	10 071(10)	1 642(5)	−1 809(9)	C(33)	7 298	477	4 945
C(2)	11 459(11)	1 122(6)	−823(11)	C(34)	8 821	295	4 936
C(3)	11 534(11)	889(6)	741(11)	C(35)	9 179	507	3 698
C(4)	9 967(12)	574(5)	737(12)	C(36)	8 012	901	2 470
C(11)	11 846(5)	3 419(3)	−2 086(5)	C(41)	5 967(6)	439(3)	−1 186(6)
C(12)	13 314	3 745	−1 991	C(42)	4 490	350	−2 479
C(13)	14 752	3 666	−657	C(43)	3 660	980	−3 309
C(14)	14 723	3 259	582	C(44)	4 305	1 700	−2 846
C(15)	13 256	2 932	487	C(45)	5 782	1 789	−1 554
C(16)	11 817	3 012	−847	C(46)	6 612	1 158	−723
C(21)	7 945(6)	3 778(3)	−2 267(5)				

Table 6 Selected bond lengths (Å) and angles (°) for complex **3**

Pt–P(1)	2.314(2)	Pt–P(2)	2.326(2)
Pt–B(1)	2.193(10)	Pt–B(2)	2.135(15)
Pt–B(3)	2.192(14)	Pt–B(2′)	2.127(25)
B(1)–B(2)	1.772(26)	B(1)–B(2′)	1.827(33)
B(3)–B(2)	1.729(21)	B(3)–B(2′)	1.509(31)
C(2)–C(3)	1.524(15)	C(1)–C(2)	1.519(12)
C(3)–C(4)	1.498(15)	C(1)–P(1)	1.828(10)
C(4)–P(2)	1.853(11)	P(1)–C(16)	1.829(6)
P(1)–C(26)	1.828(5)	P(2)–C(36)	1.828(6)
P(2)–C(46)	1.822(5)		
P(1)–Pt–P(2)	94.9(1)	B(1)–Pt–B(3)	87.1(7)
Pt–P(1)–C(1)	116.6(4)	Pt–P(2)–C(4)	113.2(3)
P(1)–C(1)–C(2)	116.0(6)	P(2)–C(4)–C(3)	114.9(7)
C(1)–C(2)–C(3)	118.1(9)	C(2)–C(3)–C(4)	115.5(7)
B(1)–Pt–B(2)	48.3(7)	B(1)–Pt–B(2′)	50.0(9)
B(3)–Pt–B(2)	47.1(6)	B(3)–Pt–B(2′)	40.9(8)
B(1)–B(2)–B(3)	119.3(10)	B(1)–B(2′)–B(3)	129.5(17)

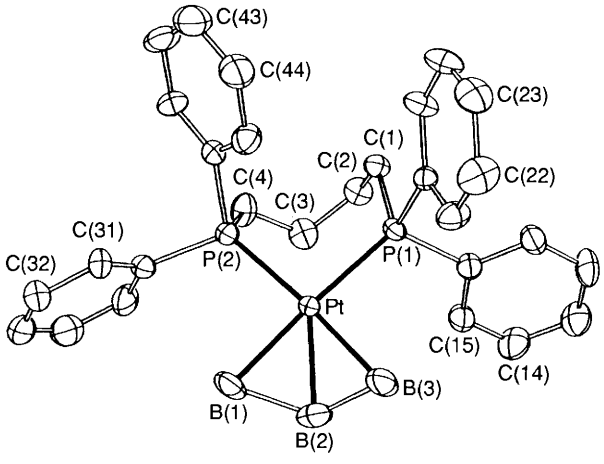

Fig. 4 Molecular structure and atom labelling for complex **3**. Hydrogen atoms were not located

a source of the (non-isolable) $[B_3H_7]^{2-}$ ligand. The preferred hydride product is the dinuclear complex $[Pt_2H_3\{(Ph_2PC_5H_4)_2Fe\}]Cl$ **6**; platinaborane **4** (Scheme 1) is formed only in *ca.* 2% yield. The $[Pt_2H_3\{(Ph_2PC_5H_4)_2Fe\}_2]^+$ cation has previously been prepared by the reaction of $[Pt(Hdmpz)\{(Ph_2PC_5H_4)_2Fe\}]^{2+}$ with $[BH_4]^-$ or by treating $[Pt_2(\mu\text{-}OH)_2\{(Ph_2PC_5H_4)_2Fe\}]^{2+}$ with $AgBF_4$.[11] Both platinum(II) precursors were initially prepared from $[PtCl_2\{(Ph_2PC_5H_4)_2Fe\}]$ with *overall* yields of $[Pt_2H_3\{(Ph_2PC_5H_4)_2Fe\}_2]^+$ with respect to the dichloride being *ca.* 21 and 41% respectively for the two routes. Our synthetic route gives only 10% of the cation (as the chloride salt **6**) but in a single and relatively easy step. The ^1H and ^{31}P NMR spectra of solutions containing the cation of **6** indicate that, even at −70 °C, the three hydride ligands are fluxional.[11] We further note that the two resonances at δ +4.31 and 4.11 assigned to the cyclopentadienyl protons[11] persist as relatively sharp signals from 293 to 210 K. We have previously discussed in detail the fluxional behaviour of $[\{(Ph_2PC_5H_4)_2Fe\}PdB_3H_7]$, namely (*i*) mutual twisting of the C_5 rings and (*ii*) inversion at the phosphorus atoms.[2] In $[\{(Ph_2PC_5H_4)_2Fe\}PdB_3H_7]$, inversion at phosphorus, but not ring twisting, is frozen out at 253 K on the 400 MHz time-scale. The data for the cation of **6** are consistent with the persistence of the inversion process at 210 K and also indicate that in solution between 298 and 210 K the average conformation at least of each ferrocene unit is an eclipsed one.

The continued fluxional behaviour of the cation of **6** in solution at low temperature prevents any conclusions being reached as regards the solid-state structure of this complex[11] and we have therefore carried out a single-crystal X-ray diffraction study of **6**. The molecular structure of the $[Pt_2H_3\{(Ph_2PC_5H_4)_2Fe\}_2]^+$ cation in **6** is shown in Fig. 5 and selected bond distances and angles are listed in Table 8. The two portions of the $[Fe(\eta^5\text{-}C_5H_4PPh_2)_2]Pt$ dimer exhibit different co-ordination geometries about the platinum(II) centres and these are viewed schematically in Fig. 6 in which the $\{Pt_2P_4\}$ core of the cation is compared with that in each of three other related cations, namely $[Pt_2H_3(PEt_3)_4]^+$,[7] $[Pt_2H_3(dppe)_2]^+$,[10,34] and $[Pt_2H_3(dbpp)_2]^+$ [dbpp = $Bu^t_2P(CH_2)_3PBu^t_2$].[6] We shall return to a comparison with these structures later. The Pt(2)–Pt(1) vector in the cation of **6** approximately bisects the angle P(1)–Pt(1)–P(2), while the {Pt(2)P(3)P(4)} unit is skewed with respect to the Pt(1)–Pt(2) vector; the angles Pt(1)–Pt(2)–P(3) and Pt(1)–Pt(2)–P(4) are 152.5(1) and 104.2(1)° respectively. The two $[Fe(\eta^5\text{-}C_5H_4PPh_2)_2]Pt$ moieties are similar to one another with ligand bite angles of 104.4(2)° at atom Pt(1) and 102.9(2)° at Pt(2). In each ferrocene unit the C_5 rings are almost exactly staggered. The cyclopentadienyl rings in the $\{Fe(\eta^5\text{-}C_5H_4PPh_2)_2\}$ unit associated with Pt(1) are parallel to each other but those associated with Pt(2) are tilted with a deviation of 5° with the inter-ring spacing decreasing towards the two phosphorus atoms. Since the two pairs of Pt–P distances are similar (Table 8), changes in the relative orientations of pairs of cyclopentadienyl rings naturally affect the P ··· P separation. The decrease from P ··· P 3.620 Å at Pt(1) to 3.571 Å at Pt(2) is consistent with the smaller P–Pt–P

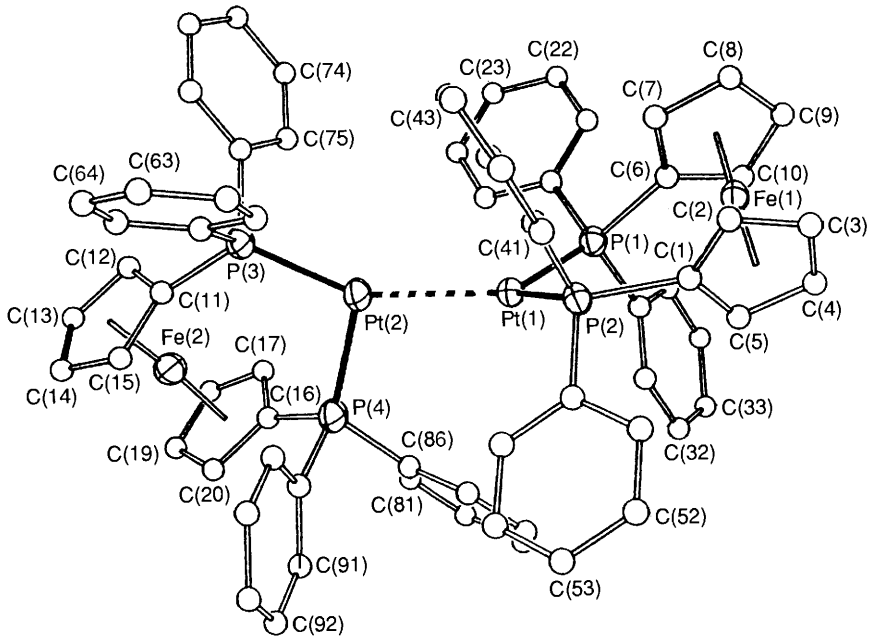

Fig. 5 Molecular structure of the $[Pt_2H_3\{(Ph_2PC_5H_4)_2Fe\}_2]^+$ cation in **6**; hydride ligands were not located

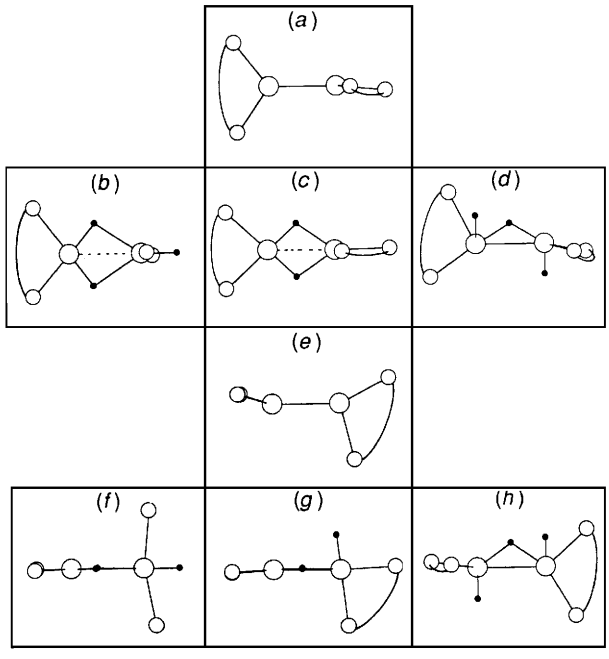

Fig. 6 Comparison of the $\{Pt_2P_4\}$ core geometries in (*a*) and (*e*) $[Pt_2H_3\{(Ph_2PC_5H_4)_2Fe\}_2]^+$, (*b*) and (*f*) $[Pt_2H_3(PEt_3)_4]^+$, (*c*) and (*g*) $[Pt_2H_3(dppe)_2]^+$ and (*d*) and (*h*) $[Pt_2H_3(dbpp)_2]^+$. Diagrams (*a*)–(*d*) are related to (*e*)–(*h*) by a 90° rotation about the Pt–Pt vector

bite angle at atom Pt(2). A number of complexes containing $[Fe(\eta^5\text{-}C_5H_4PPh_2)_2]$ as a chelate have now been structurally characterised,[2,11,35–43] and we[2] and others[36] have commented upon the interrelationship of the geometrical parameters which characterise the $\{Fe(\eta^5\text{-}C_5H_4PPh_2)_2M\}$ (**M** = transition metal) fragment. The structures of $[Pt_2(\mu\text{-}OH)_2\{(Ph_2PC_5H_4)_2Fe\}_2]^{2+}$ and $[Pt_2(\mu\text{-}CO)(\mu\text{-}H)\{(Ph_2PC_5H_4)_2Fe\}_2]^+$ are quite closely related to that of the cation of **6**, but in each previous example the two ferrocenyl ligands are symmetrically disposed.[11,43]

The hydride ligands of the cation of **6** have been located indirectly by a comparison (Fig. 6) of the $\{Pt_2P_4\}$ core structure of this cation with those of $[Pt_2H_3(PEt_3)_4]^+$,[7] $[Pt_2H_3(dppe)_2]^+$,[10,34] and $[Pt_2H_3(dbpp)_2]^+$,[6] in conjunction with a consideration of the frontier molecular orbitals of the hypothetical tetracation of **6**. Consider first the molecular geometries of the aforementioned series of monocations; each possesses both terminal and bridging hydrides. (A further related cation exhibiting additional hydride ligands is $[Rh_2(\mu\text{-}H)_3H_2\{(Ph_2PC_5H_4)_2Fe\}_2]$.[42] Although at first sight the $\{Pt_2P_4\}$ core geometries of $[Pt_2H_3(PEt_3)_4]^+$ [Fig. 6(*b*) and 6(*f*)] and $[Pt_2H_3(dppe)_2]^+$ [Fig. 6(*c*) and 6(*g*)] appear different, once the hydrides are in place, the cores are seen to be related; in $[Pt_2H_3(dppe)_2]^+$ the phosphorus atoms must reside *cis* to one another by virtue of the chelating ligand. One platinum atom is in a square-planar environment while the second exhibits trigonal-bipyramidal co-ordination.[7,10,34] The hydride positions in $[Pt_2H_3(dppe)_2]^+$ have been confirmed.[10,34] In $[Pt_2H_3(dbpp)_2]^+$ the two platinum atoms share an approximately common co-ordination geometry and the presence of one bridging and two terminal hydride ligands [Fig. 6(*d*) and 6(*h*)] has been proposed.[6] The geometry of the $\{Pt_2P_4\}$ core in the cation of **6** compares more favourably with that in $[Pt_2H_3(dppe)_2]^+$ than $[Pt_2H_3(dbpp)_2]^+$, thus implying that in the solid state it exhibits one terminal and two bridging hydrides. This places Pt(1) and Pt(2) in square-planar and trigonal-bipyramidal co-ordination environments respectively. The platinum–phosphorus distances (Table 8) are consistent with the placement of one terminal H atom *trans* to atom P(4) and bridging hydrides *trans* to P(1) and P(2) and in the equatorial plane of Pt(2) a plane which also contains atom P(3).

It has previously been suggested[10] that the structural change observed in going from $[Pt_2H_3(dppe)_2]^+$ to $[Pt_2H_3(dbpp)_2]^+$ might be due, in part, to an increase in ligand bite angle (86.0 to 99.2°). Hence, it is significant that we observe a similarity between the structures of the cation of **6** and $[Pt_2H_3(dppe)_2]^+$ despite a substantial difference in bite angle [average bite at Pt(1) and Pt(2) for $Fe(\eta^5\text{-}C_5H_4PPh_2)_2$, 103.6°; for dppe, 86.0°]. Our results would suggest that the $\{P_4Pt_2H_3\}$ geometry is controlled by the steric bulk of the phosphorus substituents, and the associated non-bonded H ··· H interactions, rather than by the bite angle of the chelating ligand.

An investigation of the nature of the frontier orbitals of a cation (or anion) can provide insight into possible sites of hydride (or proton) attack. Although the core structure of the cation of **6** is quite similar to that of $[Pt_2H_3(dppe)_2]^+$, it is not exactly the same. In order to provide additional support for the proposed hydride positions in the cation of **6** we have carried out a Fenske–Hall molecular orbital analysis of the model cation $[Pd_2H_3(PH_3)_4]^+$ and report our results in terms of (*i*)

Table 7 Atomic coordinates ($\times 10^4$) for complex **6** *

Atom	*x*	*y*	*z*	Atom	*x*	*y*	*z*
Pt(1)	853.8(7)	6 681.0(2)	6 850.6(6)	C(26)	−1 261	6 915	7 960
Pt(2)	1 362.7(8)	6 069.6(2)	7 746.0(6)	C(31)	−1 355(10)	6 897(4)	5 106(12)
Fe(1)	659(2)	7 776(1)	6 521(2)	C(32)	−2 126	6 877	4 303
Fe(2)	879(3)	5 003(1)	8 163(2)	C(33)	−3 162	6 971	4 360
P(1)	−567(4)	7 025(1)	6 967(4)	C(34)	−3 426	7 084	5 220
P(2)	2 051(4)	7 045(1)	6 339(4)	C(35)	−2 655	7 103	6 023
P(3)	2 130(5)	5 754(1)	8 984(4)	C(36)	−1 619	7 010	5 966
P(4)	900(5)	5 657(1)	6 575(4)	C(41)	4 161(14)	7 202(4)	7 107(10)
Cl(1)	−2 280(5)	6 211(2)	1 596(5)	C(42)	5 003	7 231	7 847
Cl(2)	4 309(9)	6 553(4)	11 349(8)	C(43)	4 853	7 167	8 778
Cl(3)	5 864(12)	7 067(3)	11 448(9)	C(44)	3 860	7 073	8 969
C(S1)	5 638(30)	6 626(10)	11 421(36)	C(45)	3 018	7 044	8 228
Cl(4)	−3 105(13)	5 785(4)	7 023(12)	C(46)	3 168	7 108	7 297
Cl(5)	−4 454(17)	6 349(6)	6 459(15)	C(51)	2 949(11)	7 111(3)	4 679(11)
C(S2)	−3 265(43)	6 192(15)	6 108(38)	C(52)	3 405	6 985	3 924
Cl(6)	5 326(14)	5 909(4)	13 429(13)	C(53)	3 563	6 630	3 837
Cl(7)	4 818(20)	5 289(6)	12 290(18)	C(54)	3 264	6 403	4 505
C(S3)	5 900(37)	5 405(12)	13 002(32)	C(55)	2 808	6 530	5 260
C(1)	1 638(17)	7 493(5)	5 928(14)	C(56)	2 650	6 884	5 347
C(2)	2 196(15)	7 792(5)	6 276(14)	C(61)	4 007(16)	6 098(4)	8 904(11)
C(3)	1 626(17)	8 056(5)	5 775(17)	C(62)	5 091	6 152	9 110
C(4)	761(19)	7 922(6)	5 166(16)	C(63)	5 739	5 903	9 605
C(5)	803(16)	7 559(5)	5 243(13)	C(64)	5 304	5 598	9 894
C(6)	−293(16)	7 488(5)	7 197(14)	C(65)	4 220	5 544	9 688
C(7)	553(17)	7 612(5)	7 860(11)	C(66)	3 571	5 794	9 193
C(8)	478(18)	7 986(6)	7 820(15)	C(71)	2 357(11)	5 862(4)	10 940(12)
C(9)	−350(15)	8 086(5)	7 150(13)	C(72)	1 983	5 949	11 775
C(10)	−867(17)	7 773(6)	6 741(14)	C(73)	946	6 061	11 739
C(11)	1 960(17)	5 277(5)	8 974(16)	C(74)	285	6 086	10 869
C(12)	1 381(19)	5 097(6)	9 555(15)	C(75)	659	5 999	10 034
C(13)	1 492(19)	4 747(5)	9 332(19)	C(76)	1 695	5 887	10 069
C(14)	2 171(22)	4 695(7)	8 722(19)	C(81)	−1 071(15)	5 643(4)	5 415(12)
C(15)	2 485(17)	5 036(4)	8 447(15)	C(82)	−1 799	5 743	4 633
C(16)	309(17)	5 277(5)	6 991(15)	C(83)	−1 514	5 983	3 989
C(17)	−416(18)	5 260(7)	7 620(16)	C(84)	−502	6 123	4 127
C(18)	−695(21)	4 919(8)	7 762(18)	C(85)	226	6 022	4 910
C(19)	−139(27)	4 704(6)	7 275(19)	C(86)	−58	5 783	5 554
C(20)	434(20)	4 926(7)	6 746(15)	C(91)	1 801(13)	5 327(4)	5 131(12)
C(21)	−1 641(12)	7 184(3)	8 461(11)	C(92)	2 648	5 231	4 687
C(22)	−2 142	7 111	9 238	C(93)	3 673	5 312	5 103
C(23)	−2 263	6 770	9 512	C(94)	3 852	5 490	5 963
C(24)	−1 884	6 501	9 011	C(95)	3 004	5 586	6 408
C(25)	−1 382	6 573	8 234	C(96)	1 979	5 504	5 992

* C(S1), C(S2) and C(S3) are carbon atoms of the CH_2Cl_2 solvent molecules.

the frontier-orbital properties of a hypothetical tetracation, $[Pd_2(PH_3)_4]^{4+}$ containing a core geometry equivalent to that crystallographically determined for the cation of **6**, and (*ii*) the interaction of the tetracation with three hydride ligands.

The frontier MOs of $[Pd_2(PH_3)_4]^{4+}$ include two low-lying empty orbitals (MOs 25 and 26) which are separated from the next set of unoccupied MOs by an energy gap of *ca.* 5.6 eV as shown on the left-hand side of Fig. 7. Molecular orbitals 25–27 are all metal based and the characters are represented schematically in Fig. 7 and amplitude contour plots are illustrated in Fig. 8. MO 25 [Fig. 8(*a*)] has 58% Pd(2) and 5% Pd(1) character; the single lobe that points out from Pd(2) is available to interact with a terminal hydride, but in addition the region between Pd(1) and Pd(2) is a potential site for hydride bridges. A significant feature of MO 26 is the large contribution from the Pd(1) pd hybrid orbital which lies in the plane defined by atoms Pd(1), P(1) and P(2). MO 26 comprises 61% Pd(1) and only 2% Pd(2) character and exhibits π^* character between the two metal atoms [Fig. 8(*b*)]. This orbital is ideally suited to interact with two *terminal* hydrogen atoms which lie on the side of atom Pd(1) that faces Pd(2); the nodal plane running between the two metal atoms precludes the development of a Pd–H–Pd bridge interaction. Although noticeably higher in energy than the two lowest-lying unoccupied orbitals, MO 27 [Fig. 8(*c*)] appears to be a potentially useful orbital with which incoming hydride ligands might interact. The contributions from Pd(1) and Pd(2) are 37 and 42% respectively. Thus, inspection of the low-lying empty MOs of the model tetracation $[Pd_2(PH_3)_4]^{4+}$ suggests that the core structure of this and, by analogy the tetracation of **6**, is compatible with the presence of both terminal and bridging (or semi-bridging) hydride ligands in the cation of **6**, and that a reasonable formulation for the latter is $[Pt_2(\mu\text{-}H)_2H\{(Ph_2PC_5H_4)_2Fe\}_2]^+$.

The relative roles of MOs 25, 26 and 27 in the formation of $[Pd_2(\mu\text{-}H)_2H(PH_3)_4]^+$ from $[Pd_2(PH_3)_4]^{4+}$ have been assessed. In addition, we have probed the extent to which semi- or fully bridging hydrides might be preferred; the crystallographically determined co-ordination geometries at atoms Pt(1) and Pt(2) in the cation of **6** are consistent with either type of bridging hydride. Two extreme cases have been tested and compared. In one calculation we have allowed hydrides H(1) and H(2) (defined in Fig. 7) to lie in semi-bridging positions as found experimentally in $[Pt_2H_3(dppe)_2]^+$,[10,34] and in a second calculation H(1) and H(2) lie in fully bridging positions between the two metal atoms. The correlation diagram illustrated in Fig. 7 refers to the case in which H(1) and H(2) are semi-bridging, with Pd(1)–H(1) = Pd(1)–H(2) 1.60 Å and Pd(2) · · · H(1) = Pd(2) · · · H(2) 2.20 Å.[34] The results indicate that all three MOs

25–27 are indeed involved in binding the hydride ligands to the dimetal framework. Mulliken overlap populations are listed in Table 9. For the semi-bridging model, 53% of the total overlap between the dimetal framework and atoms H(1) and H(2) involves MO 26 and this is consistent with a significant contribution from an essentially localised $\{(H_3P)_2PdH_2\}$ unit centred on Pd(1) as proposed in earlier work.[10,34] However, although we have constrained the distances Pd(1)–H(1) and Pd(1)–H(2) so as to favour this latter bonding mode, the roles of MOs 25 and 27 are non-trivial and this illustrates that bridging interactions to Pd(2) are quite well developed even in this extreme model. Table 9 also lists Mulliken overlap populations for the second model in which atoms H(1) and H(2) are moved into fully bridging sites [Pd(1)–H–Pd(2) 1.92 Å]. First, note that the total overlap between $[Pd_2(PH_3)_4]^{4+}$ and H(1) and H(2) decreases by *ca.* 17% as we go from the asymmetrical to symmetrical bridging interactions. Secondly, as expected, the role of MO 26 diminishes. Hydride H(3) is bound to Pd(2) *via* interactions with MOs 25 and 27, the former being more important as predicted in the discussion above. Although the individual overlap populations for 25-$1s_{H(3)}$ and 27-$1s_{H(3)}$ are

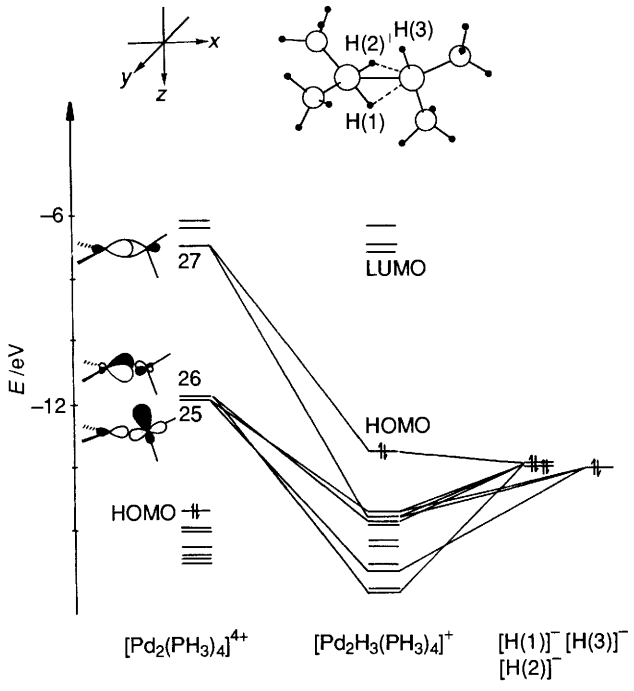

Fig. 7 Correlation diagram for the interaction of $[Pd_2(PH_3)_4]^{4+}$ with three hydride ligands to generate $[Pd_2H_3(PH_3)_4]^+$ in the geometry shown. HOMO and LUMO are the highest occupied and lowest unoccupied molecular orbitals

Table 8 Selected bond lengths (Å) and angles (°) for the $[Pt_2H_3\{(Ph_2PC_5H_4)_2Fe\}_2]^+$ cation of **6**

Pt(1)–Pt(2)	2.722(1)	Pt(1)–P(1)	2.290(5)
Pt(2)–P(3)	2.246(5)	Pt(1)–P(2)	2.291(6)
Pt(2)–P(4)	2.320(6)	P(1)–C(6)	1.846(21)
P(3)–C(11)	1.859(22)	P(2)–C(1)	1.882(20)
P(4)–C(16)	1.800(21)	P(1)–C(26)	1.840(17)
P(2)–C(46)	1.837(15)	P(1)–C(36)	1.808(15)
P(2)–C(56)	1.823(17)	P(3)–C(66)	1.837(21)
P(4)–C(86)	1.821(17)	P(3)–C(76)	1.802(15)
P(4)–C(96)	1.825(19)	C(6)–Fe(1)	2.011(22)
C(16)–Fe(2)	2.019(20)	C(1)–Fe(1)	1.958(22)
C(11)–Fe(2)	1.974(21)		
P(1)–Pt(1)–P(2)	104.4(2)	P(3)–Pt(2)–P(4)	102.9(2)
P(1)–Pt(1)–Pt(2)	127.5(1)	P(3)–Pt(2)–Pt(1)	152.5(1)
P(2)–Pt(1)–Pt(2)	124.1(1)	P(4)–Pt(2)–Pt(1)	104.2(1)
Pt(1)–P(1)–C(6)	116.5(7)	Pt(2)–P(3)–C(11)	119.9(7)
Pt(1)–P(2)–C(1)	119.7(7)	Pt(2)–P(4)–C(16)	113.6(7)
C(6)–Fe(1)–C(1)	112.2(9)	C(16)–Fe(2)–C(11)	109.5(9)

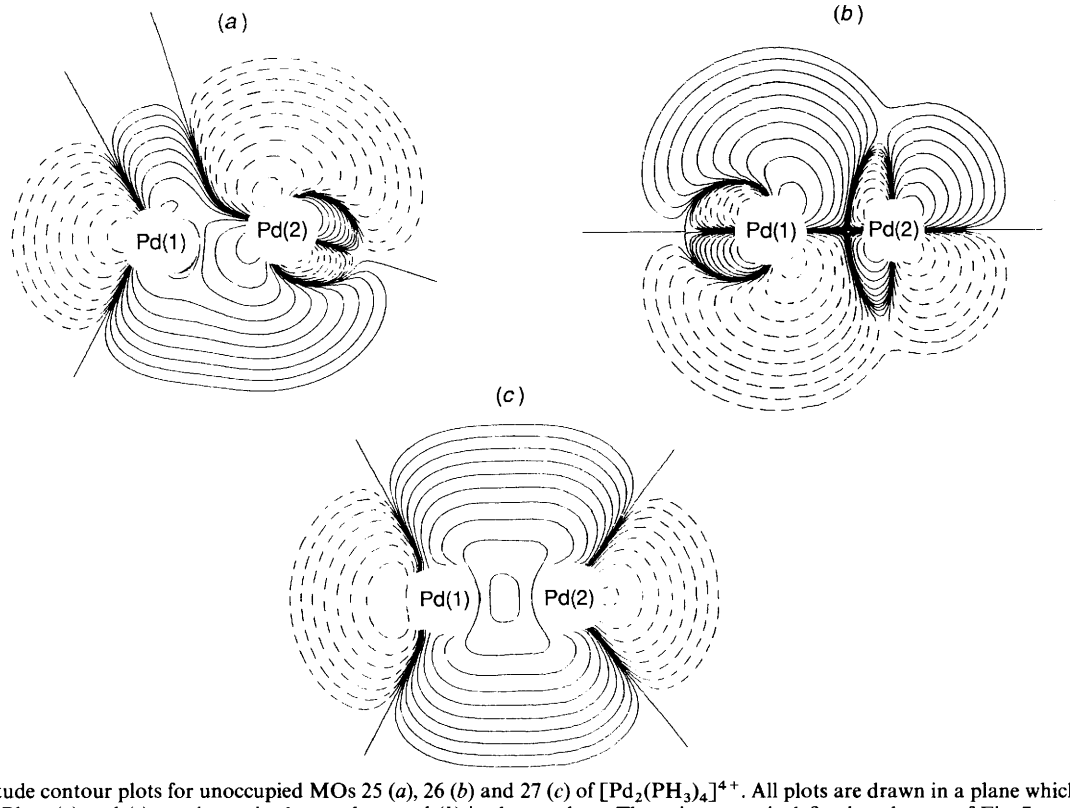

Fig. 8 Amplitude contour plots for unoccupied MOs 25 (*a*), 26 (*b*) and 27 (*c*) of $[Pd_2(PH_3)_4]^{4+}$. All plots are drawn in a plane which contains the two Pt atoms. Plots (*a*) and (*c*) are drawn in the *xz* plane and (*b*) in the *xy* plane. The axis system is defined at the top of Fig. 7; atom labelling is consistent with that in Fig. 5. Since MOs 25–27 are predominantly metal in character, eigenvector contributions from atoms other than the two Pt atoms have been omitted for clarity

Table 9 Mulliken overlap populations for the interaction of hydride ligands with the model tetracation $[Pd_2(PH_3)_2]^{4+}$ to form $[Pd_2H_3(PH_3)_2]^+$

	Mulliken overlap population with unoccupied MOs of $[Pd_2(PH_3)_2]^{4+}$			
Hydride 1s AO	MO 25	MO 26	MO 27	Total overlap population
(*i*) For semibridging hydrides: Pd(1)–H(1) = Pd(1)–H(2) 1.60 Å				
H(1) + H(2)	0.063	0.298	0.202	0.563
H(3)	0.185	—	0.093	0.278
(*ii*) For fully bridging hydrides: Pd(1)–H(1) = Pd(1)–H(2) 1.92 Å				
H(1) + H(2)	0.088	0.190	0.188	0.466
H(3)	0.178	—	0.096	0.274

affected by altering the positions of H(1) and H(2), the sum of the two is essentially unchanged.

We conclude therefore that the geometry of the $\{Pt_2P_4\}$ framework in the cation of **6** is consistent with the presence of one terminal and two bridging hydride ligands. Further, an analysis of the bonding in two extreme models in which both symmetrical and asymmetrical bridges are considered suggests that maximum metal–hydride orbital overlap is achieved if H(1) and H(2) adopt semi-bridging positions.

Acknowledgements

We thank the Royal Society for a 1983 University Research Fellowship (to C. E. H.) and the Hariri Foundation for support (to B. A. M. S.). The National Science Foundation is acknowledged for a grant towards the purchase of a diffractometer at the University of Delaware. We also thank David Wales for assistance with the MO contour-plotting program.

References

1 B. S. Haggerty, C. E. Housecroft, A. L. Rheingold and B. A. M. Shaykh, *Inorg. Chem.*, 1991, **30**, 125.
2 C. E. Housecroft, S. M. Owen, P. R. Raithby and B. A. M. Shaykh, *Organometallics*, 1990, **9**, 1617.
3 L. J. Guggenberger, A. R. Kane and E. L. Muetterties, *J. Am. Chem. Soc.*, 1972, **94**, 5665.
4 A. R. Kane and E. L. Muetterties, *J. Am. Chem. Soc.*, 1971, **93**, 1041.
5 G. Bracher, D. M. Grove, P. S. Pregosin and L. M. Venanzi, *Angew. Chem., Int. Ed. Engl.*, 1979, **18**, 155.
6 T. H. Tulip, T. Yamagata, T. Yoshida, R. D. Wilson, J. A. Ibers and S. Otsuka, *Inorg. Chem.*, 1979, **18**, 2239.
7 F. Bachechi, G. Bracher, D. M. Grove, B. Kellenberger, P. S. Pregosin, L. M. Venanzi and L. Zambonelly, *Inorg. Chem.*, 1983, **22**, 1031.
8 R. S. Paonessa and W. C. Trogler, *Inorg. Chem.*, 1983, **22**, 1038.
9 G. Minghetti, G. Banditelli and A. L. Bandini, *J. Organomet. Chem.*, 1977, **139**, C80.
10 C. B. Knobler, H. D. Kaesz, G. Minghetti, A. L. Bandini, G. Banditelli and F. Bonati, *Inorg. Chem.*, 1983, **22**, 2324.
11 A. L. Bandini, G. Banditelli, M. A. Cinellu, G. Sanna, G. Minghetti, F. Demartin and M. Manassero, *Inorg. Chem.*, 1989, **28**, 404.
12 J. D. Kennedy, *Prog. Inorg. Chem.*, 1984, **32**, 519.
13 D. F. Gaines and S. J. Hilderbrandt, *Inorg. Chem.*, 1978, **17**, 794.
14 N. N. Greenwood, J. D. Kennedy and D. Reed, *J. Chem. Soc., Dalton Trans.*, 1980, 196.
15 J. Bould, N. N. Greenwood, J. D. Kennedy and W. S. McDonald, *J. Chem. Soc., Dalton Trans.*, 1985, 1843.
16 J. Bould, N. N. Greenwood and J. D. Kennedy, *J. Organomet. Chem.*, 1983, **249**, 11.
17 M. A. Drezdon and D. F. Shriver, *Manipulations of Air Sensitive Compounds*, Wiley, New York, 1986.
18 G. E. Coates and P. Parkin, *J. Chem. Soc.*, 1963, 420.
19 G. M. Sheldrick, SHELXTL 5.1, Nicolet XRD, Madison, WI.
20 M. B. Hall and R. F. Fenske, *Inorg. Chem.*, 1972, **11**, 768.
21 E. Clementi, *J. Chem. Phys.*, 1964, **40**, 1944.
22 J. W. Richardson, M. J. Blackman and J. F. Ranochak, *J. Chem. Phys.*, 1973, **58**, 3010.
23 N. M. Kostic and R. F. Fenske, *Organometallics*, 1982, **1**, 974.
24 H.-P. Klein, U. Thewalt, H. Zettlmissl and H. A. Brune, *Z. Naturforsch., Teil B*, 1981, **36**, 1125.
25 H. Beall and C. H. Bushweller, *Chem. Rev.*, 1973, **73**, 465.
26 C. E. Housecroft and T. P. Fehlner, *Inorg. Chem.*, 1982, **21**, 1739.
27 C. J. Dain, A. J. Downs, G. S. Laurenson and D. W. H. Rankin, *J. Chem. Soc., Dalton Trans.*, 1981, 472.
28 N. P. C. Simmons, A. B. Burg and R. A. Beaudet, *Inorg. Chem.*, 1981, **20**, 533.
29 D. H. Farrar and G. Ferguson, *J. Cryst. Spectrosc. Res.*, 1982, **12**, 465.
30 B. Bovio, F. Bonati and G. Banditelli, *Gazz. Chim. Ital.*, 1985, **115**, 613.
31 W. L. Steffen and G. J. Palenik, *Inorg. Chem.*, 1976, **15**, 2432.
32 R. H. Schunn, *Inorg. Chem.*, 1970, **9**, 394.
33 C. J. Moulton and B. L. Shaw, *J. Chem. Soc., Chem. Commun.*, 1976, 365.
34 M. Y. Chiang, R. Bau, G. Minghetti, A. L. Bandini, G. Banditelli and T. F. Koetzle, *Inorg. Chem.*, 1984, **23**, 122.
35 T. Hayashi, M. Konishi, Y. Kobori, M. Kumada, T. Higuchi and K. Hirotsu, *J. Am. Chem. Soc.*, 1984, **106**, 158.
36 I. R. B. Butler, W. R. Cullen, T.-J. Kim, S. J. Rettig and J. Trotter, *Organometallics*, 1985, **4**, 972.
37 D. A. Clemente, G. Pilloni, B. Corain, B. Longato and M. Tiripicchio-Camellini, *Inorg. Chim. Acta*, 1986, **115**, L9.
38 U. Casellato, D. Ajo, G. Valle, B. Corain, B. Longato and R. Graziani, *J. Cryst. Spectrosc.*, 1988, **18**, 583.
39 S. Onaka, *Bull. Chem. Soc. Jpn.*, 1986, **59**, 2359.
40 M. I. Bruce, I. R. Butler, W. R. Cullen, G. A. Koutsantonis, M. R. Snow and R. T. Tiekink, *Aust. J. Chem.*, 1988, **41**, 963.
41 T. M. Miller, K. J. Ahmed and M. S. Wrighton, *Inorg. Chem.*, 1989, **28**, 2347.
42 F. W. B. Epstein and T. Jones, *Acta Crystallogr., Sect. C*, 1985, **41**, 365.
43 B. Longato, G. Pilloni, G. Valle and B. Corain, *Inorg. Chem.*, 1988, **27**, 956.

Received 4*th December* 1990; *Paper* 0/05455K